Migration and Trapping of Photoinjected Excess Electrons in Double-Stranded B-Form DNA But Not in Single-Stranded DNA

Vladimir Ya. Shafirovich,* Alexander Dourandin, Natalia P. Luneva, and Nicholas E. Geacintov

Chemistry Department and Radiation and Solid State Laboratory, 31 Washington Place, New York University, New York, New York 10003

Received: January 24, 1997; In Final Form: May 24, 1997[⊗]

Photoexcitation of a pyrene derivative covalently bound to double-stranded calf thymus DNA with 355 nm Nd:YAG laser pulses (fwhm = 24 ps, 50 mJ/cm^2/pulse) results in the efficient two-photon-induced ionization of the pyrenyl residues. By use of nanosecond transient absorption techniques, it is shown that the excess electrons injected into the DNA can reduce methylviologen cations (MV^{2+}) that are noncovalently bound to the DNA but not MV^{2+} in the outer aqueous solution phase. In double-stranded DNA, this reduction of MV^{2+} to $MV^{\bullet+}$ occurs via two kinetic phases, a rapid one that is complete within ≤7 ns and a slower one (200−300 ns) due to the diffusive reduction of MV^{2+} by hydrated electrons. The appearance of the first, rapid reduction phase of MV^{2+} depends on the secondary structure of the DNA, since it is observed only in the double-stranded form but not in the denatured, single-stranded form. This rapid reduction phase is entirely eliminated upon the addition of magnesium ions, which displace the positively charged MV^{2+} cations from the double-stranded DNA molecules. By variation of the concentration of MV^{2+} cations at a constant distribution of covalently bound pyrenyl residues (60 base pairs per pyrenyl residue), a mean distance of migration of excess electrons in double-stranded DNA of ca. 40 Å is estimated.

1. Introduction

The concept of efficient, one-dimensional conduction of charge carriers along the stacked bases in double-stranded B-form DNA ("molecular wire") has recently become the subject of renewed attention.[1,2] For example, long distance electron-transfer phenomena, due to long-range coupling between polynuclear aromatic donor and acceptor molecules intercalated in DNA,[3−9] and metal complexes covalently linked to oligonucleotides[1a,10,11] have been studied. The overlap between the low-lying π-orbitals can mediate base-to-base electron or hole transfer, thus leading to long-distance charge transfer. Excess charge carriers, e.g., excess electrons or holes in DNA that can be produced by ionizing radiation, photochemical processes, or electrochemical reactions are also believed to migrate in DNA.[12−15] Studies of excess electron migration in DNA have been mostly restricted to EPR and conductivity measurements in matrices at low temperatures and in the solid state (for recent reviews, see refs 12 and 13). Studies at ambient temperatures in aqueous solutions have focused mainly on the generation of hydrated electrons by radiolysis and their diffusion and reactions with electron traps intercalated within double- stranded DNA molecules.[14,15] In these experiments, the time scales of trapping by DNA molecules of the hydrated electrons generated in the bulk of the solution, are typically in the microsecond domain; therefore, studies of electron migration phenomena within the DNA molecules were limited to longer time scales only.

Here, we report on the direct spectroscopic observation of the trapping of excess electrons injected directly into double-stranded DNA. The excess electrons are generated by the two-photon ionization of a pyrene derivative[16] bound covalently to double-stranded DNA using 355 nm picosecond laser pulses. A fraction of these excess electrons is readily trapped by methylviologen molecules (MV^{2+}) noncovalently bound to the same DNA duplexes within ≤7 ns. This effect is dependent on the DNA secondary structure, since it is not observed in denatured, predominantly single-stranded DNA. The rapid capture of the excess electrons in double-stranded DNA is in sharp contrast to the slower, diffusion-controlled kinetics of electron capture from the bulk of the solution by MV^{2+} observed in the case of denatured DNA.

2. Experimental Section

The highly polymerized calf thymus DNA was obtained from Worthington Biochemical Corp. (Freehold, NJ) and purified by phenol extraction and exhaustive dialysis. The purified DNA in 20 mM phosphate buffer (pH 7) was characterized by a melting temperature of 70.9 °C and a hyperchromicity of 39 ± 4%, which agrees well with published values.[17] The benzo[*a*]-pyrene derivative 7*r*,8*t*-dihydroxy-*t*9,10-epoxy-7,8,9,10-tetrahydrobenzo[*a*]pyrene (BPDE) was reacted with the purified DNA to generate adducts with covalently bound residues with a pyrenyl aromatic ring system, as described previously.[18] After extensive purification of the DNA reacted with BPDE by ether extraction and after exhaustive dialysis against 20 mM phosphate buffer (pH 7) to remove the tetraol hydrolysis products of BPDE, the ratio of covalently bound BPDE molecules per DNA base pairs was determined spectrophotometrically[19] to be 1:60. The extinction coefficients used were ϵ_{348} = 29 000 cm^{-1} M^{-1} for covalently bound BPDE and ϵ_{258} = 6700 cm^{-1} M^{-1} for DNA. The major product formed from the reaction of BPDE with native DNA is associated with the covalent *trans* addition of the exocyclic amino group of guanosine residues in DNA to the C10 ring-opened position of BPDE.[20,21] The melting characteristics of the BPDE-modified DNA were not measurably different from those of the unmodified DNA. The BPDE-modified DNA was denatured by heating at 90 °C (10 min) followed by rapid cooling in an ice−water mixture.

The methylviologen was obtained from Fisher Scientific (Pittsburgh, PA) and purified by precipitation from methanol solution by the addition of acetone.

* To whom correspondence should be addressed.

[⊗] Abstract published in *Advance ACS Abstracts,* July 1, 1997.

S1089-5647(97)00308-8 CCC: $14.00 © 1997 American Chemical Society

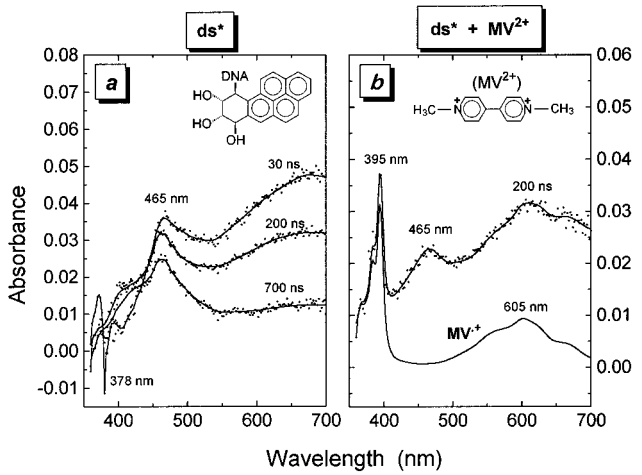

Figure 1. Transient absorbance spectra of double-stranded BPDE-modified DNA (2 mM) in deoxygenated 20 mM phosphate buffer (pH 7) solutions, where (a) $[MV^{2+}] = 0$ and (b) $[MV^{2+}] = 68$ μM, and λ(excitation) = 355 nm at ~50 mJ cm^{-2} pulse^{-1}, measured with different delay times Δt after the excitation laser pulse. The solid line (b, lower part) is a normalized spectrum of $MV^{\bullet+}$ radical cations generated by chemical reduction of MV^{2+} by $N_2S_2O_4$ ($[MV^{2+}] = 0.1$ mM, 50 mM sodium borate buffer solution, pH 9).

The transient absorption spectra were recorded by a kinetic spectrometer (7 ns response time) using a mode-locked Quantel International YaG-501 Nd:YAG laser (355 nm, fwhm = 24 ps, 3 mJ/pulse, 6 mm × 1 mm spot, 20 Hz) as an excitation source, a 100 W xenon flash lamp as the probe, and a Hamamatsu R928 phomultiplier coupled to a Tektronix TDS 620 digital oscilloscope. Following excitation with the 355 nm laser pulses, the transient absorbance was recorded at a particular wavelength over a time interval of 1000 ns; the resolution was 2 ns per data point, and 50 successive decay curves were accumulated and averaged in order to improve the signal/noise ratio. By advancing the wavelength settings of a McPherson monochromator stepwise at 2 nm intervals, an array of 200 decay curves in the 350−750 nm wavelength range was obtained and stored in the memory of a computer. The transient absorption spectra at different time intervals after the excitation, Δt, were constructed by sampling the amplitudes of each of the 200 decay curves at the same time interval Δt. All experiments, including data collection and analysis, were controlled by an IBM PC computer.

Fluorescence emission spectra were measured by conventional excitation at 350 nm in a Hitachi Model MPF-2A fluorescence spectrometer (Perkin-Elmer Corp., Norwalk, CT) that was interfaced with an IBM PC computer for data collection and analysis.

The concentration of the DNA used in all experiments was identical (2 mM in nucleotide concentration), and the concentration of covalently bound pyrenyl residues was 17 μM. The aqueous solutions were placed in a 8 mm quartz cell that was degassed on a vacuum pump line (0.1 Pa, ca 10^{-3} Torr). This level of degassing was sufficient to prevent the trapping of electrons by O_2. Laser flash photolysis experiments were performed at 20 °C. Under these conditions, sample decomposition did not exceed 10%.[18,22,23]

3. Results and Discussion

Photoioniztion of Pyrenyl Residues in BPDE-Modified DNA. Typical transient absorption spectra of BPDE-modified DNA in aqueous solution recorded at delay times $\Delta t = 30$, 200, and 700 ns after the actinic 355 nm picosecond laser pulse excitation are shown in Figure 1a. In the 30 ns transient absorption spectrum, the minimum at 378 nm is associated with the residual fluorescence of the pyrenyl moieties. At all three Δt values, a maximum at 465 nm is observed, which is attributed to the pyrenyl radical cation formed by the photoionization of pyrenyl residues.[16,24] The maximum of the pyrenyl radical cation is red-shifted by 10 nm in comparison with that of the radical cation ($\lambda_{max} = 455$ nm) of 7,8,9,10-tetrahydroxytetrahydrobenzo[*a*]pyrene (BPT) in aqueous solution in the absence of DNA.[16] This 10 nm red-shift is attributed to the electronic interactions between the pyrenyl derivative radical cation and neighboring nucleic acid bases in covalently linked BPDE−DNA adducts. A structureless absorption band from about 500 to 700 nm is observed in the 30−200 ns time range, which corresponds to the well-known transient absorption spectrum of hydrated electrons with a broad maximum near 700 nm.[25] These observations indicate that the transient absorption spectrum of BPDE−DNA, even at $\Delta t = 30$ ns, is a superposition of the transient absorption spectra of pyrenyl radical cations and hydrated electrons. Contributions to the transient absorption spectra of pyrenyl singlet excited states (for ^{1}BPT, $\lambda_{max} = 480$ nm[26]) seem to be negligible most likely because of efficient quenching by nucleic acid bases. This is evident from the short mean lifetimes, ~3.0 ns, of pyrenyl residue singlet excited states in BPDE−DNA adducts (this mean lifetime is the weighted average of a 1.4 and a 5.7 ns component with relative amplitudes of 63 and 37%, respectively[18]).

Addition of methylviologen (MV^{2+}) to the aqueous BPDE−DNA adduct solutions exerts a pronounced effect on the transient absorption spectra (Figure 1b); a narrow absorption band with a maximum at 395 nm and a broader absorbance maximum near 605 nm, both due to the methylviologen radical cation ($MV^{\bullet+}$), the reduction product of MV^{2+}, appear.[27] For comparison, the absorption spectrum of $MV^{\bullet+}$, generated by the chemical reduction of MV^{2+} by $Na_2S_2O_4$ in the absence of DNA under anaerobic conditions, is shown by the solid line in the lower part of Figure 1b.

Although the molar extinction coefficent of $MV^{\bullet+}$ at 395 nm is greater by a factor of 3 than at 605 nm, the characteristic maximum at 605 nm was used in all subsequent analyses because the pyrenyl fluorescence signal below 430 nm interfered with the transient absorbance measurements (Figure 1a). In the 500−700 nm region, changes in the transient absorbance were recorded at Δt intervals as short as 10 ns after the 355 nm excitation laser pulses.

The formation of $MV^{\bullet+}$ occurs only upon photoionization of pyrenyl residues and the concomitant appearance of hydrated electrons. At low excitation energies[16] (<10 mJ cm^{-2} pulse^{-1}), neither photoionization of pyrenyl residues[24] nor the formation of hydrated electrons or MV^{2+} occurs to any measurable extent on time scales of ≤7 ns. These results indicate that electron transfer from the pyrenyl singlet excited states to MV^{2+} is not occurring under these conditions of relatively low-energy laser pulse excitation.

Kinetics of Reduction of Methylviologen in Double-Stranded and in Single-Stranded DNA. The transient absorption spectra of double-stranded (ds*) and single-stranded (ss*) DNA solutions (the asterisks refer to BPDE-modified DNA) in the presence of 68 μM methylviologen ($[N_{bp}]/[MV^{2+}] = 15$, where $[N_{bp}]$ is the molar concentration of DNA base pairs) were determined at different time delays, Δt, following the laser flash. A typical absorption spectrum measured at $\Delta t = 200$ ns is depicted in Figure 1b (upper curve). The solid curve is a least-squares fit of the $MV^{\bullet+}$ and hydrated electron spectra in which the relative contributions of each to the total absorption spectrum were treated as adjustable parameters. The relative absorbance

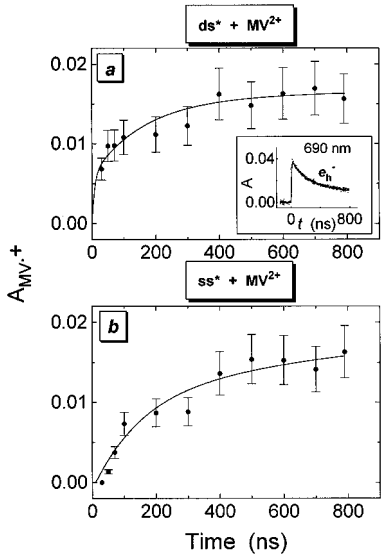

Figure 2. Kinetics of the rise in the absorbance of $MV^{\bullet+}$ radical cations ($A_{MV^{\bullet+}}$) deduced from transient absorption spectra determined at different delay times after a laser excitation flash (see text for details). The deoxygenated solutions contained double-stranded (ds*) and single-stranded (ss*) BPDE-modified DNA and 68 μM methylviologen. Other conditions are as in Figure 1. The solid lines are fits of sums of two or three exponential terms to the experimental data points with time constants deduced from the decay curves of the absorbance of hydrated electrons (a typical decay curve measured at 690 nm is shown in the insert in the upper panel). The details of the fitting procedures, as well as the values of the associated fitting parameters, are described in more detail in the Supporting Information.

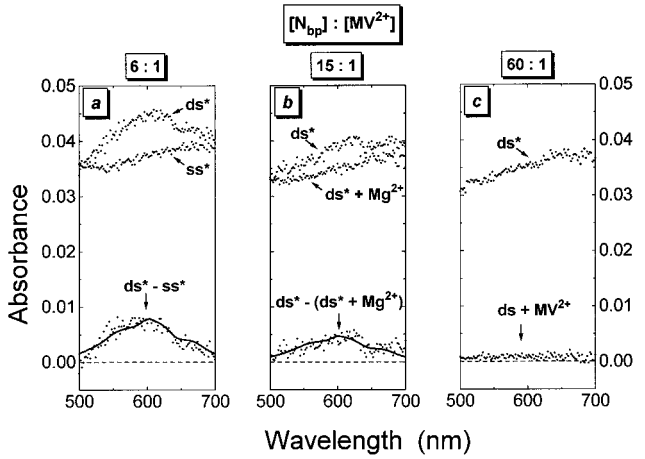

Figure 3. Effect of MV^{2+} concentration on the transient absorption spectra of double-stranded (ds*) and single-stranded (ss*) BPDE−DNA in deoxygenated aqueous solutions: (a) $[MV^{2+}] = 170$ μM; (b) $[MV^{2+}] = 68$ μM; (c) $[MV^{2+}] = 17$ μM (upper part) and 170 μM (lower part). The spectra were measured with a delay time of $\Delta t = 30$ ns after the excitation laser pulse (the molar concentration ratios $[N_{bp}]/[MV^{2+}]$ ratios are 6:1, 15:1, and 60:1, respectively. Other conditions are as in Figure 1.

due to the reduced $MV^{\bullet+}$ radical ions ($A_{MV^{\bullet+}}$) at different delay times Δt (Figure 2) was estimated in this manner by decomposing the different transient absorption spectra into their $MV^{\bullet+}$ and hydrated electron components. The absorption spectrum of $MV^{\bullet+}$ was determined by reducing MV^{2+} with $Na_2S_2O_4$ (lower portion of Figure 1b), while the absorption spectra of the hydrated electrons above 550 nm were obtained from transient absorption spectra determined as shown in Figure 1a.

The contributions to the total transient absorption spectra of the $MV^{\bullet+}$ radical ions were determined for solutions of BPDE-modified double-stranded and single-stranded DNA for 11 representative transient absorption spectra in the time interval of $\Delta t = 30-700$ ns (Figure 2) chosen from a total array of 400 spectra. There is a marked dependence of the efficiency of reduction of MV^{2+} to $MV^{\bullet+}$ on the secondary structure of DNA. In double-stranded BPDE-modified DNA, there is a prompt (ca. 7 ns) rapid rise in the $MV^{\bullet+}$ absorbance (Figure 2a). However, in denatured DNA, there is no rapid phase in the reduction of MV^{2+}, and the concentration of $MV^{\bullet+}$ rises more slowly and monotonically within the $\Delta t = 0-800$ ns time interval (Figure 2b). A similar slow phase in the reduction kinetics of MV^{2+} following the initial rapid rise is observed also in double-stranded DNA (Figure 2a). The time scale for the slow kinetics of formation of $MV^{\bullet+}$ in Figure 2 is, within experimental error, equal to those of the decay of the hydrated electrons monitored by transient absorption at 690 nm (a typical decay curve of hydrated electrons is shown in the insert in Figure 2a). A more detailed description of the comparison of the kinetics of the $A_{MV^{\bullet+}}$ curves and the decay of hydrated electron is provided in the Supporting Information section. The coincidence of the rates of disappearance of the hydrated electrons and the rate of appearance of $MV^{\bullet+}$ suggests that the latter are formed via diffusive bimolecular encounters between hydrated electrons and MV^{2+}. The reduction of methylviologen by hydrated electrons in aqueous solutions has been observed previously[28−30] and was not further investigated in this work.

Double Helical Structure of DNA is Critical for the Intermolecular Reduction of Methylviologen. The interpretation of the rapid kinetic phase in the reduction of MV^{2+} observed in double-stranded but not in single-stranded DNA (Figure 2) is supported by the transient absorbance spectra observed at different Δt values and by the effects of magnesium ions on these spectra. The transient absorption spectra in the 500−700 nm region at three typical molar concentration ratios $[N_{bp}]/[MV^{2+}] = 6$, 15, and 60 are depicted in Figure 3.

The binding constant of MV^{2+} to native DNA has been reported[3] to be 1.8×10^5 M^{-1}; therefore, more than 95% of the added MV^{2+} is assumed to be bound to the DNA under the conditions of the experiments of parts a and c of Figure 3. The transient absorption spectra obtained with double- and single-stranded BPDE-modified DNA with $[N_{bp}]/[MV^{2+}] = 6$ are strikingly different in the case of the double-stranded and the denatured, single-stranded DNA ($\Delta t = 30$ ns, Figure 3a). In the case of ds* DNA, a transient absorption spectrum with a maximum at ~605 nm is observed, whereas in the case of ss* DNA, only the background due to the hydrated electrons is observed. The difference between these spectra (ds* − ss*) is in excellent agreement with the absorption spectrum of free $MV^{\bullet+}$ (the spectrum generated by chemical reduction of MV^{2+} with $Na_2S_2O_4$ in the absence of DNA, as shown by the solid line in the lower part of Figure 3a). It is especially noteworthy that the appearance of the $MV^{\bullet+}$ spectrum within ≤7 ns of the excitation pulse occurs only in the case of the double-stranded, but not in the case of single-stranded, BPDE-modified DNA under otherwise identical conditions.

The amplitude of the $MV^{\bullet+}$ signal, measured at the early time delay of $\Delta t = 30$ ns, decreases with decreasing concentration of MV^{2+} (Figure 3b) and is no longer apparent at a $[N_{bp}]/[MV^{2+}]$ ratio of 60 (Figure 3c, upper portion). There is no discernible transient absorption spectrum due to $MV^{\bullet+}$ in the BPDE-modified single-stranded DNA at this low concentration of MV^{2+}. When identical experiments are carried out with *unmodified* double-stranded DNA (ds) in the presence of MV^{2+}, there are no detectable transient absorbance signals (Figure 3c,

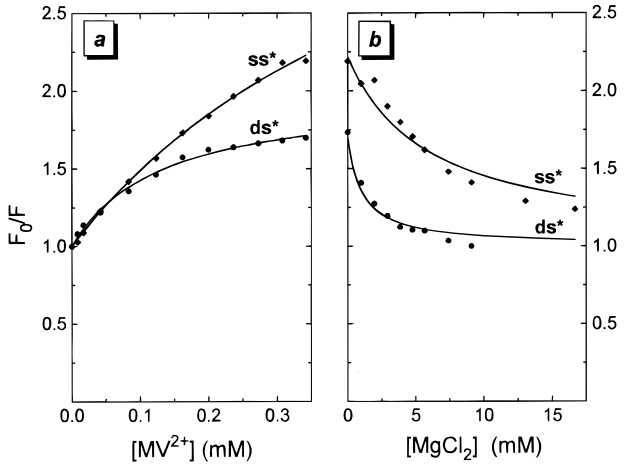

Figure 4. Stern−Volmer plots of fluorescence yield (F) ratios, F_0/F, as a function of (a) methylviologen concentration and (b) magnesium chloride concentrations in air-equilibrated solutions of double-stranded (ds*) and single-stranded (ss*) BPDE−DNA: (a) $[Mg^{2+}] = 0$; (b) $[MV^{2+}] = 340$ μM. The solid lines are shown for visualization. Conditions are as in Figure 1.

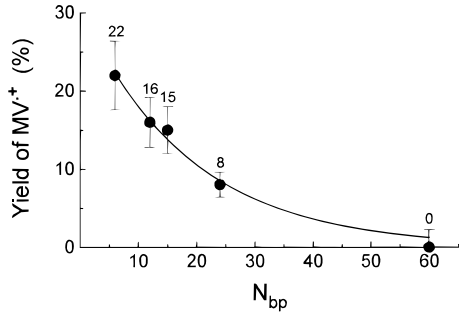

Figure 5. Relative yield of $MV^{\bullet+}$ radical cations, ($[MV^{\bullet+}]/([MV^{\bullet+}] + [e_h^-]$), calculated at a delay time of $\Delta t = 30$ ns after the excitation laser pulse, as a function of the average number of DNA base pairs per MV^{2+} molecules noncovalently bound to DNA, $[N_{bp}]/[MV^{2+}]$. The yields of $[MV^{\bullet+}]$ were calculated by fitting the sum of the known $MV^{\bullet+}$ absorption plus the absorption spectrum of hydrated electrons, e_h^-, using the experimental transient absorption spectra at $\Delta t = 30$ ns (see text for details). The solid line represents a fit of the normalized function, $\exp(-\Delta N_{bp}/N_e)$ with $N_e = 24$ base pairs and ΔN_{bp} being the mean distance between the BPDE residues and MV^{2+} ions, to the experimental data points.

lower part). These results indicate that ionization of DNA[12,13] or water[31] does not occur under our conditions of laser excitation.

Effects of Mg^{2+} Ions on Transient Absorption Spectra Due to the Reduction of MV^{2+}. Addition of excess magnesium ions to aqueous solutions of double-stranded BPDE-modified DNA tends to displace the positively charged MV^{2+} ions that are associated with the double helix into the outer solution. In Figure 3b, it is shown that the addition of 10 mM Mg^{2+} ions eliminates the signal due to the reduction of MV^{2+}. Again, the difference between the transient absorption spectra of double-stranded BPDE−DNA at $[Mg^{2+}] = 0$ and at $[Mg^{2+}] = 10$ mM shows that the ds* − (ds* + Mg^{2+}) transient absorption spectra coincides with the $MV^{\bullet+}$ spectrum (solid line, Figure 3b).

Quenching of the Fluorescence by MV^{2+} and the Effects of Mg^{2+} Ions. Methylviologen readily quenches the fluorescence of BPT in aqueous solution (in the absence of DNA) by both dynamic and static mechanisms, i.e., via bimolecular complex formation (data not shown). The fluorescence of pyrenyl residues in BPDE-modified single- and double-stranded DNA are also quenched by methylviologen (Figure 4a); as the MV^{2+} concentration is increased, the fluorescence yield decreases. Since the mean fluorescence lifetime of pyrenyl residues in covalent BPDE−DNA adducts is ca. 3 ns,[18] only DNA-bound MV^{2+} can quench the fluorescence of pyrenyl residues at concentrations of $[MV^{2+}] \lesssim 0.4$ mM. The Stern−Volmer plots are nonlinear in both double-stranded and denatured DNA and curve toward the horizontal axis. The fluorescence of the pyrenyl residues is quenched with approximately similar efficiencies in ss* and ds* DNA at MV^{2+} concentrations below ~0.07 mM, but the quenching at higher MV^{2+} concentrations is less efficient in ds* than in ss* DNA. The downward-sloping Stern−Volmer quenching plots associated with BPDE-modified DNA adducts have been observed previously using acrylamide as a quencher[32,33] and have been attributed to heterogeneities in fluorescence lifetimes and adduct conformations, each with different accessibilities to the fluorophore quenchers.[18] Although the shapes of the Stern−Volmer plots are not the focus of this work, it is interesting to note that the singlet excited states of the pyrenyl residues are quenched by MV^{2+} ions in both ss* and ds* DNA but that only the ds* DNA exhibits the rapid reduction phase of the MV^{2+} ions upon laser pulse excitation. At low fluences of excitation (<10 mJ cm^{-2} $pulse^{-1}$), we did not observe any reduction of the MV^{2+} ions accompanying the quenching of the fluorescence (data not shown). These results may be understood in terms of the observations of Rodgers and co-workers[30] who showed that nonfluorescent ground-state complexes are formed between MV^{2+} and pyrenyl residues bound covalently to poly(methacrylic acid); the fluorescence of the pyrenyl residues is quenched by MV^{2+} via an electron transfer mechanism within <20 ps of excitation, but radical ion products are not observed presumably because of their rapid recombination in these bimolecular complexes.[30] A similar mechanism probably accounts for the quenching of the fluorescence of the pyrenyl residues in BPDE-modified DNA (Figure 4) and a lack of formation of $MV^{\bullet+}$ radical cation products at low laser pulse fluences.

Upon addition of Mg^{2+}, the positively charged MV^{2+} cations are displaced from the ss* and ds* DNA, and the fluorescence quenching effect due to MV^{2+} disappears completely, especially in the case of ds* DNA ($F_0/F \rightarrow 1.0$ as the magnesium ion concentration is increased to 5 mM and above; Figure 4b). These results indicate that both the quenching of the fluorescence by MV^{2+} and the reduction of MV^{2+} to $MV^{\bullet+}$ by excess electrons observed only at high laser pulse fluences (Figure 3) are processes mediated by MV^{2+} cations that are bound to the double-stranded DNA rather than by MV^{2+} ions present in the surrounding aqueous solution.

Migration of Excess Electrons along the DNA Helix. The prompt reduction of MV^{2+} induced by photoionization of pyrenyl residues in BPDE-modified double-stranded DNA can be explained in terms of the migration of excess electrons from their site of generation toward MV^{2+} cations bound to the DNA. This hypothesis is supported by a number of observations. First, the reduction of MV^{2+} occurs rapidly (≤7 ns) in double-stranded DNA but not in denatured DNA. Second, the addition of Mg^{2+} cations, which displaces MV^{2+} ions noncovalently bound to the DNA double helixes, abolishes the fast rise in the concentration of the reduced form of methylviologen, $MV^{\bullet+}$. These observations suggest that excess electrons injected into the DNA by two-photon ionization of pyrenyl residues migrate along the DNA duplex and are trapped by methylviologen cations associated with the double helix.

The relative efficiency of prompt $MV^{\bullet+}$ formation ($\Delta t = 30$ ns) as a function of $[N_{bp}]/[MV^{2+}]$, the average number of DNA base pairs between MV^{2+} molecules noncovalently bound to DNA, is shown in Figure 5. The relative absorbances due to

$MV^{\bullet+}$ ($A_{MV^{\bullet+}}$) and hydrated electrons ($A - A_{MV^{\bullet+}}$, where A is the overall absorbance) were calculated by decomposing the transient absorption spectra recorded at $\Delta t = 30$ ns into their $MV^{\bullet+}$ and hydrated electrons components; the relative concentrations of $MV^{\bullet+}$ and hydrated electrons were determined from $A_{MV^{\bullet+}}$ and $A - A_{MV^{\bullet+}}$ by using the molar extinction coefficients $\epsilon_{605} = 1.37 \times 10^4$ M^{-1} cm^{-1} ($MV^{\bullet+}$)[27] and $\epsilon_{700} = 1.9 \times 10^4$ M^{-1} cm^{-1} (hydrated electrons).[24b] The concentration of covalently bound BPDE residues (60 DNA base pairs per BPDE residue) is constant in these experiments. The solid line is a plot of the function $\exp(-N_{bp}/N_e)$, where the attenuation parameter N_e is equal to 24 base pairs. A characteristic value of the distance over which excess electrons can migrate in double-stranded DNA can be estimated assuming that the MV^{2+} cations are randomly distributed. Ground-state complexes between DNA bound pyrenyl residues and MV^{2+} are not expected to yield any radical ion products because of rapid ion radical recombination;[30] therefore, the assumption that the mean estimated distances between MV^{2+} ions are not affected by nearest neighbor or other complex formation is reasonable. The prompt ($\leq$7ns) generation of reduced methylviologen characterized by $N_e = 24$ (Figure 5) suggests that the average distance between pyrenyl residue and methylviologen is typically $\sim$12 base pairs. Hence, assuming that the trapping efficiency of excess electrons by MV^{2+} is efficient, a typical excess electron migration distance of $\sim$40 Å in double-stranded DNA can be deduced.

Our results, as well as those of Richards et al.,[24] indicate that the energy of two 355 nm photons (7.0 eV) is sufficient to ionize the pyrenyl residues and to generate excess electrons in the surrounding aqueous phase and within the DNA molecule. The migration of excess electrons along the DNA double helix can be viewed in terms of charge transport in a "conduction band" resulting from the overlapping orbitals of adjacent DNA bases.[34,35] However, the long-distance transfer of excess electrons within the DNA conduction band is likely to be limited by the escape of the excess electrons into the aqueous phase or into the primary and secondary shells of hydration surrounding duplex DNA (for a review, see ref 36). The lack of electronic conductivity of dehydrated DNA and the dramatic increase in conductivity upon hydration supports the hypothesis that excess electron migration occurs in the DNA hydration layer.[37] Assuming that such hydrated electrons undergo a one-dimensional diffusion, a diffusion length of 60 Å within $\Delta t =$ 7 ns (the response time of our experimental apparatus) can be estimated from the diffusion coefficient of the hydrated electron, $D = 4.9 \times 10^{-5}$ cm^2/s,[38] and the relationship $r = (D\Delta t)^{1/2}$. This value of r is in close agreement with our experimental value of 40 Å. Thus, our experimental results are consistent with a mechanism of migration of hydrated electrons along the double-stranded DNA helix. However, the response time of our kinetic spectrometer (7 ns) does not exclude a faster mechanism of migration, e.g., the rapid migration of excess electrons within the overlapping π-orbitals of the stacked DNA bases on subnanosecond time scales.

Another potentially important mechanism of migration of excess electrons may involve detrapping and trapping of the electrons by nucleic acid bases in which reduction is followed by protonation.[39] DNA nucleosides, predominantly dC and to a lesser extent dT, can be easily reduced by excess electrons.[12,13] The dC and dT electron adducts, even in their protonated forms, have more negative redox potentials ($E = -1.09$ V vs NHE, pH 8.4−8.8)[39] than methylviologen ($E° = -0.44$ V vs NHE)[40] and thus can easily reduce[41] MV^{2+}. In principle, the trapping of excess electrons by dC and dT can affect the migration distance. However, in this work, we made no attempts to estimate the contribution of this mechanism to the distance dependence of the reduction of MV^{2+}.

Finally, the migration of excess electrons within DNA might be occurring by a combination of several mechanisms discussed above. Whatever the mechanism of migration, our results clearly indicate that the double-stranded secondary structure is critical to the observation of long-distance excess electron migration in DNA.

Acknowledgment. This work was supported by the Department of Energy, Grant FGO2-86ER060405 from the Office of Health and Environmental Research. We are grateful to the referee for some important suggestions that helped to improve this publication.

Supporting Information Available: More detailed discussion of absorbance due to reduction of MV^{2+} and two figures illustrating absorption spectra of double- and single-stranded BPDE−DNA, hydrated electrons, and $MV^{\bullet+}$ radical cations (5 pages). Ordering information is given on any current masthead page.

References and Notes

(1) (a) Murphy, C. J.; Arkin, M. R.; Jenkins, Y.; Gatlia, N. D.; Bossmann, S. H.; Turro, N. J.; Barton, J. K. *Science* **1993**, *262*, 1025. (b) Arkin, M. R.; Stemp, E. D. A.; Holmlin, R. E.; Barton, J. K.; Hörmann, A.; Olson, E. J. C.; Barbara, P. F. *Science* **1996**, *273*, 475. (c) Hall, D. B.; Holmlin, R. E.; Barton, J. K. *Nature* **1996**, *382*, 731.

(2) Meade, T. J. In *Metal Ions in Biological Systems*; Sigel, A., Sigel, H., Eds.; Marcel Dekker: New York, 1996; p 453.

(3) Fromherz, P.; Rieger, B. *J. Am. Chem. Soc.* **1986**, *108*, 5361.

(4) Atherton, S. J. In *Light in Biology and Medicine*; Douglas, R. H., Moan, J., Dal'Acqua, F., Eds.; Plenum: New York, 1988; Vol.1, p 77.

(5) Baguley, B. C.; Le Bret, M. *Biochemistry* **1984**, *23*, 937.

(6) Brun, A. M.; Harriman, A. *J. Am. Chem. Soc.* **1992**, *114*, 3656.

(7) Barton, J. K.; Kumar, C. V.; Turro, N. J. *J. Am. Chem. Soc.* **1986**, *108*, 6391.

(8) Purugganan, M. D.; Kumar, C. V.; Turro, N. J.; Barton, J. K. *Science* **1988**, *241*, 1645.

(9) Arkin, M. R.; Stemp, E. D.; Turro, C.; Turro, N. J.; Barton, J. K. *J. Am. Chem. Soc.* **1996**, *118*, 2267.

(10) Jenkins, Y.; Barton, J. K. *J. Am. Chem. Soc.* **1992**, *114*, 8736.

(11) Meade, T. J.; Kayyem, J. F. *Angew. Chem., Int. Ed. Engl.* **1995**, *34*, 352.

(12) (a) Becker, D.; Sevilla, M. D. *Adv. Radiat. Biol.* **1993**, *17*, 121. (b) Razskazovskii, Y.; Swarts, S. G.; Falcone, J. M.; Taylor, C.; Sevilla, M. D. *J. Phys. Chem. B* **1997**, *101*, 1460.

(13) O'Neill, P.; Fielden, E. M. *Adv. Radiat. Biol.* **1993**, *17*, 53.

(14) Anderson, R. F.; Patel, K. B.; Wilson, W. R. *J. Chem. Soc., Faraday Trans.* **1991**, *87*, 3739.

(15) (a) Beach, C.; Fuciarelly, A. F.; Zimbrick, J. D. *Radiat. Res.* **1994**, *137*, 385. (b) Fuciarelly, A. F.; Sisk, E. C.; Zimbrick, J. D. *Int. J. Radiat. Biol.* **1994**, *65*, 409.

(16) Shafirovich, V. Ya.; Levin, P. P.; Kuzmin, V. A.; Thorgeirsson, T. E.; Kliger, D. S.; Geacintov, N. E. *J. Am. Chem. Soc.* **1994**, *116*, 63.

(17) Fiel, R. J.; Howard, J. C.; Mark, E. H.; Datta Gupta, N. *Nucleic Acids Res.* **1979**, *6*, 3093.

(18) Geacintov, N. E.; Zinger, D.; Ibanez, V.; Santella, R.; Grunberger, D.; Harvey, R. G. *Carcinogenesis* **1987**, *8*, 925.

(19) Xu, R.; Birke, S.; Carberry, S. E.; Geacintov, N. E.; Swenberg, N. E.; Harvey, R. G. *Nucleic Acids Res.* **1992**, *20*, 6167.

(20) Meehan, T.; Straub, K. *Nature* **1979**, *277*, 410.

(21) Cheng, S. C.; Hilton, B. D.; Roman, J. M.; Dipple, A. *Chem. Res. Toxicol.* **1989**, *2*, 334.

(22) Boles, T. C.; Hogan, M. E. *Proc. Natl. Acad. Sci. U.S.A.* **1984**, *81*, 5623.

(23) Li, B.; Mao, B.; Liu, T.-M.; Xu, J.; Dourandin, A.; Amin, S.; Geacintov, N. E. *Chem. Res. Toxicol.* **1995**, *8*, 396.

(24) Richards, J. T.; West, G.; Thomas, J. K. *J. Phys. Chem.* **1970**, *74*, 4137.

(25) (a) Hart, E. J.; Boag, J. W. *J. Am. Chem. Soc.* **1962**, *84*, 4090. (b) Buxton, G. V.; Greenstock, C. L.; Helman, W. P.; Ross, A. B. *J. Phys. Chem. Chem. Ref. Data* **1988**, *17*, 2420.

(26) Shafirovich, V. Ya.; Courtney, S. H.; Ya, N.; Geacintov, N. E. *J. Am. Chem. Soc.* **1995**, *117*, 4920.

(27) Watanabe, T.; Honda, K. *J. Phys. Chem.* **1982**, *86*, 2616.
(28) Farrington, J. A.; Ebert, M.; Land, E. *J. Chem. Soc., Faraday Trans 1*, **1978**, *74*, 665.
(29) Aikawa, M.; Turro, N. J.; Ishigo, K. *Chem. Phys. Lett.* **1994**, *222*, 197.
(30) (a) Stramel, R. D.; Nguyen, C.; Webber, S. E.; Rodgers, M. A. J. *J. Phys. Chem.* **1988**, *92*, 2934. (b) Shand, M. A.; Rodgers, M. A. J.; Webber, S. E. *Chem. Phys. Lett.* **1991**, *177*, 11.
(31) For review, see the following. Crowell, R. A.; Bartels, D. M. *J. Phys. Chem.* **1996**, *100*, 17940.
(32) Hogan, M. E.; Dattagupta, N.; Whitlock, J. P., Jr. *J. Biol. Chem.* **1981**, *256*, 4504.
(33) Underman, O.; Lycksell, P.-O.; Gräslund, A.; Astlind, T.; Ehrenberg, A.; Jernström, B.; Tjernéld, F.; Nordén, B. *Cancer Res.* **1983**, *43*, 1851.
(34) Felts, A. K.; Pollard, W. T.; Friesner, R. A. *J. Phys. Chem.* **1995**, *99*, 2929.
(35) Priyadarshy, S.; Risser, S. M.; Beratan, D. N. *J. Phys. Chem.* **1996**, *100*, 17678.
(36) Berman, H. M. *Curr. Opin. Struct. Biol.* **1991**, *1*, 423.
(37) (a) Van Lith, D.; De Haas, M. P.; Warman, J. M.; Hummel, A. *J. Chem. Soc., Faraday Trans. 1* **1986**, *82*, 2933. (b) Warman, J. M.; de Haas, M. P.; Rupprecht, A. *Chem. Phys. Lett.* **1996**, *249*, 319.
(38) Schmidt, K. H.; Han, P.; Bartels, D. M. *J. Phys. Chem.* **1992**, *96*, 199.
(39) Steenken, S.; Telo, J. P.; Novais, Candeias, L. P. *J. Am. Chem. Soc.* **1992**, *114*, 4701.
(40) Hünig, S.; Gross, J.; Schenk, W. *Liebigs Ann. Chem.* **1973**, 324.
(41) Steenken, S. *Chem. Rev.* **1989**, *89*, 503. .